CDF/PUB/CDF/CDFR/924

PHYSICS AT THE TEVATRON COLLIDER

Giorgio Bellettini
Dipartimento di Fisica della Università, Pisa
INFN, Sezione di Pisa

ABSTRACT : An outline is given of the on-going experimental program at the Fermilab Tevatron Collider, and of the first physics results as of October 1987.

Talk given at the 8th International Conference on
"Physics in Collisions", Capri, Italy, Octorber 9-12 1988.

The Tevatron had a first run at $\sqrt{s}$ = 1.8 TeV between late 1986 and May 1987. The machine worked with three on three bunches. The top luminosity at intersection BØ was about $2 \cdot 10^{29}$ cm^{-2} s^{-1}, and the integrated luminosity by the CDF experiment at that intersection was approximately 30 nb^{-1}.

There are four crossing points equipped with experiments at the Tevatron: E713 searches for magnetic monopoles and highly ionizing particles[1]: this experiment is presently in progress. Experiment E735[2] employs a multiparticle magnetic spectrometer at $\vartheta \sim 90°$ and studies particle spectra (π/ K/P at $p_T \leq 1.4$ GeV/c) and charged multiplicity to catch signals of the onset of quark-gluon plasma. The first results show the charged particle $\langle p_T \rangle$ as a function of multiplicity density in pseudorapidity, as shown in Fig. 1[3]. A phase transition would possibly be indicated by a flattening of $\langle p_T \rangle$ (plasma temperature) above some n_{ch}-density value (energy density). No significant indication for such an effect is seen in the data.

E710[4] studies elastic scattering down to the Coulomb interpherence region. They employ a set of trigger counters and mini-drift chambers in several re-entrant "Roman pots" left and right of the intersection. As of now, a preliminary value for the cross-section slope is obtained[5]. Fig. 2 shows a sketch of the pot assembly, and illustrates how elastic events are sorted out by requiring collinearity between the two final state tracks (displacements from the beams, left and right of the event vertex, should be in the same proportion to distance). Fig. 3 shows preliminary cross-section data at $|t| \geq 0.02$ (GeV/c)^2. One finds in the fit $b = 17.2 \pm 1.3$ (GeV/c)$^{-2}$.

CDF (Collider Detector at Fermilab)[6] is the only general-purpose full-coverage detector at the Collider, to be complemented by a second one at intersection DØ in 1991. This detector was designed and built by a U.S., Japanese and Italian Collaboration[7]. A sketch of the detector, whose components are described in detail in ref.(6), is shown in Fig. 4. Around the beam-crossing point, at angles larger than ~ 4°, events are first sampled by a set of VTPC's (Vertex Time-Projection Chambers), where charged tracks are seen as short (≥ 14 cm depending on production angle) straight prongs. Despite the 1.5 Tesla solenoid

field, the lever of arm is not sufficient to let tracks bend usefully for momentum measurement in this detector. The VTPC information is used for finding the z-location of the event vertex, and for measuring the charged multiplicity. The reconstruction efficiency of isolated tracks is fair at $p_T > 50$ MeV/c, and is $\geq 95°$ at $p_T \geq 100$ MeV/c and pseudorapidity $|\eta| \leq 2.5$. The z-coordinate of tracks is measured in separate azimuthal octants, within which a $r\varphi$ measurement is made with an accuracy of ~ 0.5 mm. The z-coordinates of tracks are determined with a resolution which varies depending on polar angle θ, and at the VTPC boundary is typically ~ 0.5 mm at $\vartheta = 90°$ and ~ 1 mm at $\vartheta = 10°$. The two-track separation also depends on ϑ. For two tracks in the same azimuthal φ-angle octant, the minimum separation is about 5 mm at $\vartheta = 90°$ and grows with decreasing angle. Although this detector produces useful qualitative data, it is a delicate task to work out all correction to the measured track rates and to assess the systematic errors. Fig. 5 shows preliminary uncorrected pseudorapidity distribution of charged tracks in inclusive events, at $|\eta| < 2.5$, showing an approximate plateau[8]. On compairing with the ISR and with CDF data taken at the SPS Collider energy ($\sqrt{s} = 630$ GeV)(*), one sees that the particle density grows with energy. The $\sqrt{s} = 630$ GeV data agree approximately with UA5. The preliminary CDF result at $|\eta| = 0$ is $dn/d\eta = 2.9 \pm 0.4$ at $\sqrt{s} = 630$ GeV, and $dn/d\eta = 4.0 \pm 0.4$ at $\sqrt{s} = 1800$ GeV. A more solid result is the cross-section ratio $\sigma(1800)/\sigma(630) = 1.33 \pm 0.04$ (at $\eta = 0$)[8].

Radially outside behind the VTPC's, a cylindrical Central Tracking Chamber measures charged particle momenta. The tracking code has good efficiency ($\geq$ 99%) at $p_T \geq 400$ MeV/c and $|\eta| \leq 1.0$. Some inclusive data based on the CTC information is shown in Fig. 6[9]. The invariant single particle cross-section at $\eta = 0$ is seen to develop a larger p_T-tail when increasing energy between $\sqrt{s} = 630$ GeV and $\sqrt{s} = 1800$ GeV. A fit as $E\, d^3\sigma/d^3p = A\, p_0^n/(p_T + p_0)^n$ gives $A = 0.45 \pm 0.01$ barn $\cdot$ GeV^2, $p_0 = 1.29 \pm 0.02$ GeV and $n = 8.26 \pm 0.08$ at $\sqrt{s} = 1800$ GeV. By integrating this cross-section between $p_T = 0$ and $p_T = \infty$, one gets $\langle p_T \rangle$. This

(*) Inclusive inelastic data were taken by CDF using a left-right beam-beam trigger, whose acceptance was computed to be 43 ± 6 mb at 1800 GeV, and 34 ± 3 mb at 630 GeV.

measurement would be subject to a considerable systematic error if based on the CTC information alone, since one estimates that more than 50% of the charged flux gets lost below the $p_T \cong 400$ MeV/c cut. However, the total flux is measured down to $p_T \sim 50$ MeV/c in the inner VTPC's, with a loss of only a few percents. Thus, the VTPC information allows to reduce the systematic error in the extrapolation at $p_T = 0$. The resulting $\langle p_T \rangle$[9] is shown in Fig. 7 together with lower energy data. One sees an increase of $\langle p_T \rangle$ with energy faster than lnS.

The excellent tracking and momentum resolution of the CTC allows an easy detection of K_S^o's[8],[10]. Fig. 8 shows an invariant mass distribution of all pairs of opposite charge, after simple cuts on p_T ($p_T > 250$ MeV/c), on the distance of minimum approach D of each track to the event vertex ($D_{1,2} > 2$ mm), and on the goodness of the two-track vertex in transverse r-φ space ($\chi^2 < 5$). One sees a clear K_o signal. This analysis allows to derive the K_o production cross-section in inclusive events, as shown in Fig. 9[10]. If one fits the invariant cross-section as $E\, d^3\sigma/d^3p = A\, p_o^n/(p_T + p_o)^n$ with p_o fixed at $p_o = 1.3$ GeV/c as in inclusive charged production, one finds $A = 41.9 \pm 7.7$ mb GeV^{-2}, and $n = 7.65 \pm 0.22$. From this data one can estimate that the K/charged ratio reaches ~ 30% at $p_T \geq 3$ GeV/c.

Sorrounding the CTC and the magnet solenoid, CDF features a refined electromagnetic and hadron calorimeter (Fig. 4, ref. 6). Plastic scintillator is used as sensitive medium in the central and endwall calorimeters ($\theta \geq 30°$), while proportional gas chambers with inductive pad read-out are used in the plug ($10° < \theta \leq 30°$) and in the forward ($2° \leq \theta \leq 10°$) calorimeters. Scintillator plates and chamber pads are shaped and assembled into projective towers all-over.

The 1987 CDF run concentrated on hard physics. The previously described lnS data amounted to a minor amount of the collected data. The trigger was in general an OR of a large total-E_T trigger ($\Sigma E_T >$ 20, 30, 40 and 45 GeV depending on Collider luminosity) aiming at jet physics,of a large electromagnetic E_T trigger ($\sum_{c.m.} E_T > 7$, 15 GeV) and a large ($E_T > 5$ GeV) electromagnetic cluster trigger aiming at W/Z and new heavy particle physics. Muon drift chambers on the rear side of the central calorimeters were also operational. These provided a muon

trigger, by requiring fast outs to be in coincidence with stiff tracks in corresponding sectors of the CTC. The muon trigger has worked well and provided useful data to run-in the system, but in 1987 this was too incomplete to produce real physics.

From the large E_T triggers, jets as well as electrons were easily seen after simple cuts. Fig. 10 shows an example of jets in the "lego" η-φ plot. Events show up like this by displaying just the e.m. and hadron tower pulser heights, with no corrections. Although jets are easy to detect, a much more delicate task is to derive their correct energy and to correct the observed rate to derive the parton-level rate. The cluster algorithm integrates the cluster in the η-φ space over $R = \sqrt{\Delta\eta^2 + \Delta\varphi^2} < 0.6$[11] to get the total jet signal. Since the calorimeter response to single charged tracks is found to be weaker when the track energy decreases below 10 GeV (most of the test beam calibration data was taken on a 50 GeV pion beam, where the nominal calibration factor converting pulse-height into energy was defined), the measured signal must be corrected for this important non- linearity. The single particle response, averaged over the impact point on calorimeter towers, was obtained in test beam data at $p_{ch} > 10$ GeV, and with isolated tracks in minimum bias events at $p_{ch} < 10$ GeV. This response is shown in Fig. 11[12]. The Isajet Montecarlo + CDF simulators were tuned to reproduce the observed prong multiplicity and momentum distribution of jets in CDF[13], and then used to predict the calorimeter response to jets after allowing for non-linear response to single prongs. Some minor correction is brought in by the underlying event[14] (order GeV, negative) and by the energy lost outside the clustering cone[15] (order GeV, positive). The overall correction factor[16] can be approximately written as $E_{jet} = 1.12\ E_{measured}{}^{+11.35}$ GeV, and amounts to a positive correction of 35% for 20 GeV clusters ($\pm$ 13% error) and of 14% for 250 GeV clusters ($\pm$ 5% error).

The observed E_T distribution of jet rate is the result of the true distribution at production folded into the CDF jet energy resolution. Using the Montecarlo + simulator, this resolution is known and the original distribution can be unfolded[17]. Small acceptance corrections are also applied[18], and the jet rate is normalised to the luminosity ($\pm$ 15% uncertain at this stage[19]) to get the cross-

section. While acceptance corrections are small, the correction for smearing effects amounts to + 68% at E_T = 30 GeV, and to + 12% at E_T = 250 GeV.

The inclusive cross-section at y ~ 0 is shown in Fig. 12[20]. In addition to the E_T- dependent statistical and systematic errors shown in the plot, there is an additional ± 34% normalization uncertainty. The leading order QCD predictions also have an appreciable theoretical uncertainty, as indicated as a continuos band. In Fig. 13 the same data are shown in parton-model invariant form. The apparent scaling violation between CERN and Fermilab is unfortunately not significant in view of the normalization errors present both in the CDF data and in the CERN data. However, significant scaling violation, as expected in QCD, is seen between ISR and Fermilab. CDF checked wether the large $p_\perp$-tail of the jet cross-section is consistent with a component flatter than QCD, which would be indicative of parton sub-structures. Following Eichten et al.[21] and similarly to what UA1 has done[22], we parametrised the additional contact-term as a four-fermion colour - singlet isoscalar interaction of unit strength with an associated energy scale $\wedge$. A comparison to the data at E_T > 150 GeV with an extrapolated QCD fit at 50 < E_T < 150 GeV, showed that the data is consistent with no contact-interaction, and that $\wedge$ > 700 GeV at 90% c.l.. The cross-section assuming $\wedge$ = 400 GeV (the UA1 limit) is shown in Fig. 14. The fact that we see no jet at E_T > 250 GeV plays a key role in determing the present lower limit for $\wedge$.

The two jet production angular distribution in their c.m.s., as well as the same distribution for the leading jet in three jet events, were studied and compaired with QCD. Although many amplitudes contribute even at the first α_s-order in QCD, their angular behaviour is roughly the same and is like in Rutherford scattering. This behaviour is shown as a continous curve in Fig. 15. The two jet data are split into samples of different minimum M_{jj}, since larger M_{jj} events can be measured down to smaller scattering angle with smaller corrections[23]. Both for two and three jet events the distributions are fully consistent with QCD.

Four jet events are being studied[24] in a search for double parton interactions in one and the same collision, which would possibly be mixed four-jets events generated by single interactions with bremsstrahlung of two hard gluons. Double

parton interactions would be indicated by the transverse momentum being balanced two-by-two by jet pairs in the event. A variable is built indicating how well E_T-balancing can be obtained in an event, with an optimal choice of two-by-two jet-pairing (in absissa in Fig. 16). The expected event distribution as a function of this variable in double collisions can be reasonably predicted by randomly merging two independent two-into-two parton-parton interactions in Isajet (dotted curve in Fig. 16). The QCD double gluon-radiation distribution in a preliminary calculation is found to be much broader (broken curve in Fig. 16). The data falls somewhere in between. Since the available QCD calculation is not really reliable, no fit in terms of two components was attempted. The only thing that one can say for the time being is that the double parton interaction is not dominating the four jet sample.

A study of jet fragmentation is possible in CDF[25], where the total energy is derived from the calorimeter information, and the charged prong momenta from the reconstructed tracks in the CTC. This measurement is being performed aiming eventually at distinguishing jet flavour - besides checking scaling violations, as expected in QCD. The reconstruction efficiency is studied versus jet internal rapidity both by injecting additional tracks into the jet core and by reconstructing simulated jets. A large and rather flat efficiency is found, ranging from ~ 95% at the internal jet-prong rapidity $y_{jet} = 2$ to ~ 85% at $y_{jet} \cong 5$. As a preliminary result one derives the charged multiplicity in the jet-core ($y_{jet} > 2$). A plot of this multiplicity as a function of di-jet mass allows a comparison with e^+e^- data, as shown in Fig. 17. The core multiplicity is found to grow consistently and more than linearly with energy from lower energy e^+e^- data to CDF.

Missing E_T events are being studied in CDF, in particular as a tool for discovering SUSY particles[26]. In a minimal SUSY model in which there is one degenerate squark and similarly one gluino, and the photino is the lightest (and stable) SUSY particle, the final state signatures would be jets and missing E_T, no matter wether the gluino is heavier of the squark or viceversa. There is an appreciable efficiency for CDF to detect one, two or even more such jets. In a first approach, we have looked for events with one jet and missing E_T ("monojets"). After requesting central jets ($|\eta| < 1$), events are rejected when there is an

indication of a second jet approximately opposite in azimuth. Indeed, a dangerous source of "monojets" are jet pairs in which one if the two jets is poorly measured by the detector. After applying suitable cuts to the jet parameters to define jets of good quality, only 9 events are left in the 1987 sample, whose maximum missing E_T is 38 GeV. The expected distributions for a couple of choices of gluino and squark masses - around 80 GeV and 100 GeV - are shown as an illustration in Fig. 18. If m(gluino) = 90 GeV and m(squark) = 80 GeV, for example, one would expect ~ 14 events at $E_T > 38$ GeV, where none is sees. Possible systematic errors in jet detection efficiency and errors in energy calibration should be taken into account when one wants to derive lower limits to mass of SUSY particles. From this preliminary analysis, the results shown in Fig. 19 are derived. The 90% confidence lower limits on the masses depend on wether the gluino is heavier than the squark or viceversa, being the available final states different in the two cases. The limits which were before of approximately 40 GeV at UA1[27] are now approximately 75 GeV.

Conclusions.

CDF has begun producing interesting data in lnS, electroweak and jet physics, and in searching for new heavy particles. This was possible with an integrate luminosity of ~ 30 nb^{-1} collected in 1987, and with a partially incomplete detector. Great hopes are attached to the next 1988-1989 run, when a much higher statistics is expected ($L > 1$ pb^{-1}) with a fully operational detector.

References.

1) Proposal for a Search for Highly Ionizing Particles for the DØ Area at Fermilab - K.Kinoshita and P.B.Price, Fermilab Collider Proposal (E713).
2) Search for a Deconfined Quark-Gluon Phase of Strongly Interacting Matter in pbar-p Interactions at $\sqrt{s} \cong 2$ TeV - L.J. Gutay et al., Fermilab Collider Proposal (E735).
3) Quark Gluon Plasma - Overview and Experimental Results from E735 - Frank Turkot for the FNAL E-735 Collaboration, presented at the 7th Topical Workshop on Antiproton-Proton Collisions, Fermilab, June 1988.
4) N.A.Amos et al., Nucl. Instr. and Meth. in Phys. Res. A 252, 263 (1986).
5) N.A.Amos et al., Phys. Rev. Lett. 61, 525 (1988).
6) The Collider Detector at Fermilab - A compilation of articles reprinted from Nucl. Instr. and Meth. in Phys. Res. A.
7) The CDF Collaboration (Physics Run 1987): F.Abe, D.Amidei, G.Apollinari, G.Ascoli, M.Atac, P.Auchincloss, A.R.Baden, A.Barbaro-Galtieri, V.E.Barnes, F.Bedeschi, S.Belforte, G.Bellettini, J.Bellinger, J.Bensinger, A.Beretvas, P.Berge, S.Bertolucci, S.Bhadra, M.Binkley, R.Blair, C.Blocker, J.Bofill, A.W.Booth, G.Brandenburg, D.Brown, A.Byon, K.L.Byrum, M.Campbell, R.Carey, W.Carithers, D.Carlsmith, J.T.Carroll, R.Cashmore, F.Cervelli, K.Chadwick, T.Chapin, G.Chiarelli, W.Chinowsky, S.Cihangir, D.Cline, D.Connor, M.Contreras, J.Cooper, M.Cordelli, M.Curatolo, C.Day, R.Del Fabbro, M.Dell'Orso, L.De Mortier, T.Devlin, D.Di Bitonto, R.Diebold, F.Dittus, A.Di Virgilio, J.E.Elias, R.Ely, S.Errede, B.Esposito, B.Flaugher, E.Focardi, G.W.Foster, M.Franklin, J.Freeman, H.Frisch, Y.Fukui, A.F.Garfinkel, P.Giannetti, N.Giokaris, P.Giromini, L.Gladney, M.Gold, K.Goulianos, C.Grosso-Pilcher, C.Haber, S.R.Hahn, R.Handler, R.M.Harris, J.Hauser, T.Hessing, R.Hollebeek, L.Holloway, P.Hu, B.Hubbard, P.Hurst, J.Huth, H.Jensen, R.P.Johnson, U.Joshi, R.W.Kadel, T.Kamon, S.Kanda, D.Kardelis, I.Karliner, E.Kearns, R.Kephart, P.Kesten, H.Keutelian, S.Kim, L.Kirsch, K.Kondo, U.Kruse, S.E.Kuhlmann, A.T.Laasanen, W.Li, T.Liss, N.Lockyer, F.Marchetto, R.Markeloff, L.A.Markosky, P.Mc Intyre, A.Menzione, T.Meyer, S.Mikamo, M.Miller, T.Mimashi, S.Miscetti, M.Mishina, S.Miyashita, N.Mondal, S.Mori, Y.Morita, A.Mukherjee, C.Newman- Holmes, L.Nodulman, R.Paoletti, A.Para, J.Patrick, T.J.Phillips, H.Piekarz, R.Plunkett, L.Pondrom, J.Proudfoot, G.Punzi, D.Quarrie, K.Ragan, G.Redlinger, J.Rhoades, F.Rimondi, L.Ristori, T.Rohaly, A.Roodman, A.Sansoni, R.Sard, V.Scarpine, P.Schlabach, E.E.Schmidt, P.Schoessow, M.H.Schub, R.Schwitters, A.Scribano, S.Segler, M.Sekiguchi, P.Sestini, M.Shapiro, M.Sheaff, M.Shibata, M.Shochet, J.Siegrist, P.Sinervo, J.Skarha, D.A.Smith, F.Snider, R.St.Denis, A.Stefanini, Y.Takaiwa, K.Takikawa, S.Tarem, D.Theriot, A.Tollestrup,

G.Tonelli, Y.Tsay, F.Ukegawa, D.Underwood, R.Vidal, R.G.Wagner, R.L.Wagner, J.Walsh, T.Watts, R.Webb, T.Westhusing, S.White, A.Wicklund, H.H.Williams, T.Yamanouchi, A.Yamashita, K.Yasuoka, G.P.Yeh, J.Yoh, and F.Zetti.

Institutions:

Argonne National Laboratory, Argonne, Illinois 60439

Brandeis University, Waltham, Massachusetts 02254

University of Chicago, Chicago, Illinois 60637

Fermi National Accelerator Laboratory, Batavia, Illinois 60510

Laboratori Nazionali di Frascati, Istituto Nazionale di Fisica Nucleare, Frascati, Italy

Harvard University, Cambridge, Massachusetts 02138

University of Illinois, Urbana, Illinois 61801

National Laboratory for High Energy Physics (KEK), Tsukuba-gun, Ibaraki-ken 305, Japan

Lawrence Berkeley Laboratory, Berkeley, California 94720

University of Pennsylvania, Philadelphia, Pennsylvania 19104

Istituto Nazionale di Fisica Nucleare, University and Scuola Normale Superiore, 56100 Pisa, Italy

Purdue University, West Lafayette, Indiana 47907

Rockefeller University, New York, New York 10021

Rutgers University, Piscataway, New Jersey 08854

Texas A&M University, College Station, Texas 77843

University of Tsukuba, Ibaraki 305, Japan

University of Wisconsin, Madison, Wisconsin 53706

8) Minimum Bias Physics at $\sqrt{s}$ = 1.8 TeV - CDF Collaboration, presented by Adam Para at the 7th Topical Workshop on Antiproton-Proton Collisions, Fermilab, June 1988.

9) Transverse Momentum Distribution of Charged Particles Produced in pbarp Interactions at $\sqrt{s}$ = 630 and 1800 GeV - F.Abe et al. (the CDF Collaboration), Phys. Rev. Lett. 61, 1819 (1988).

10) Strange Particle Production at the Tevatron Collider with CDF - The CDF Collaboration, presented by F.Bedeschi at the 24th Rencontre de Moriond: Progress in Hadron Physics, March 1989.

11) Cluster Algorithms and their Performance - R.Carey et al., CDF note CDF 605.

12) Response of the Central Calorimeter to Low Energy Charged Particles - S.Behrends et al., CDF note, CDF 583.

13) Checks of the CDFSIM Central Calorimeter Simulation - S.Behrends and S.Kuhlmann, CDF note, CDF 684.

14) Underlying Event Energy in Clusters - B.Flaugher and S.Kuhlmann, CDF note, CDF 685.

Figure Captions.

Fig. 1 Average transverse momentum of negative prongs versus multiplicity density in pseudorapidity (E-735[3]).

Fig. 2 E710 layout (top), and left-right correlation of track displacement, showing evidence for elastic events.

Fig. 3 E710 t-distribution of elastic events in proton-antiproton scattering at $\sqrt{s}$ = 1800 GeV[5].

Fig. 4 A cut-away view through one half of CDF.

Fig. 5 Preliminary uncorrected pseudorapidity distributions measured at CDF[8].

Fig. 6 Single charged particle inclusive cross-section for rapidity $|y| < 1.0$ and fitted curves with p_0 fixed at 1.3 GeV/c[9].

Fig. 7 Energy dependence of $\langle p_T \rangle$, from the ISR to CDF.

Fig. 8 Invariant mass-distribution of opposite charge particle pairs measured in the CDF CTC showing the K_0 peak[8][10].

Fig. 9 Invariant cross-section for K_0-production (CDF 1987 data)[10].

Fig. 10 Typical CDF jet event, as seen in the "Lego plot".

Fig. 11 Energy dependence of response of CDF central calorimeter to charged isolated hadrons.

Fig. 12 The CDF inclusive central jet cross-section at $\sqrt{s}$ = 1800 GeV as a function of transverse energy compaired to a range of QCD predictions.

Fig. 13 Scaled jet cross-section[20] as a function of $x_t = 2\,E_t/\sqrt{s}$ for the UA1, UA2 and CDF experiments. Also shown are QCD predictions.

Fig. 14 CDF jet cross-section at $\eta = 0$, as a function of E_T. The large E_T tail is compaired to the prediction if a contact term[21] with $\wedge$ = 400 GeV (UA1 lower limit) is added to the QCD contribution.

Fig. 15 Angular dependence of two jets cross-section in the jet cms (CDF data from 1987 run, ref.[22]).

Fig. 16 Distribution of four-jet events versus the "paired missing E_T significance" (CDF preliminary data from 1987 run[23]). The data is compaired to expectation from overlap of two-jet events and from an approximate QCD Montecarlo of double gluon bremsstrahlung.

Fig. 17 Prong multiplicity in jet core ($\eta_j > 2$) as measured in CDF (preliminary result from 1987 run[24], compaired to e^+e^- data at lower dijet masses).

Fig. 18 Expected E_T distribution of monojet events for squarks and gluinos of masses around 100 GeV, compaired to 1987 CDF data[25].

Fig. 19 Preliminary SUSY limits as derived from the CDF 1987 data.

15) Central Jet Energy Corrections due to Clustering Effects - S.Kuhlmann, CDF note, CDF 687.
16) Central Jet Energy / Momentum Corrections - S.Kuhlmann et al., CDF note, CDF 686.
17) Unsmearing the single Jet Inclusive Distribution - R.Harris, CDF note, CDF 606.
18) Acceptance Issues for the Inclusive Jet Cross-Section - S.Kuhlmann, CDF note, CDF 711.
19) Luminosity Monitoring and Beam-Beam Counter Performance - T.M.Liss, CDF note, CDF 552.
20) Measurement of the Inclusive Jet Cross-Section in pbarp Collisions at $\sqrt{s}$ = 1.8 TeV - F.Abe et al. (the CDF Collaboration), to appear in Phys. Rev. Lett., 1989.
21) E.Eichten et al., Phys. Rev. Lett. 50, 811 (1983).
22) G.Arnison et al., The UA1 Collaboration, Phys. Lett. 172B, 461 (1986).
23) Dijet Angular Distributions from pbarp Collider - F.Abe et al. (the CDF Collaboration), to be submitted to Phys. Rev. Lett..
24) Dijet Angular Distribution and Multijet Topology at $\sqrt{s}$ = 1.8 TeV - the CDF Collaboration, presented by James F.Patrick at the 7th Topical Workshop on Proton-Antiproton Coll.Phys., Fermilab, June 1988.
25) Jet Fragmentation Properties at CDF - the CDF Collaboration, presented by Bradley Hubbard at the 7th Topical Workshop on Proton-Antiproton Coll.Phys., Fermilab, June 1988.
26) Limits on the Masses of Supersymmetric Particles from 1.8 TeV pbarp Collisions - the CDF Collaboration, presented by Jim Freeman at the 7th Topical Workshop on Proton-Antiproton Coll.Phys., Fermilab, June 1988.
27) C.Albajar et al., The UA1 Collaboration, Phys. Lett. 198B, 261 (1987).

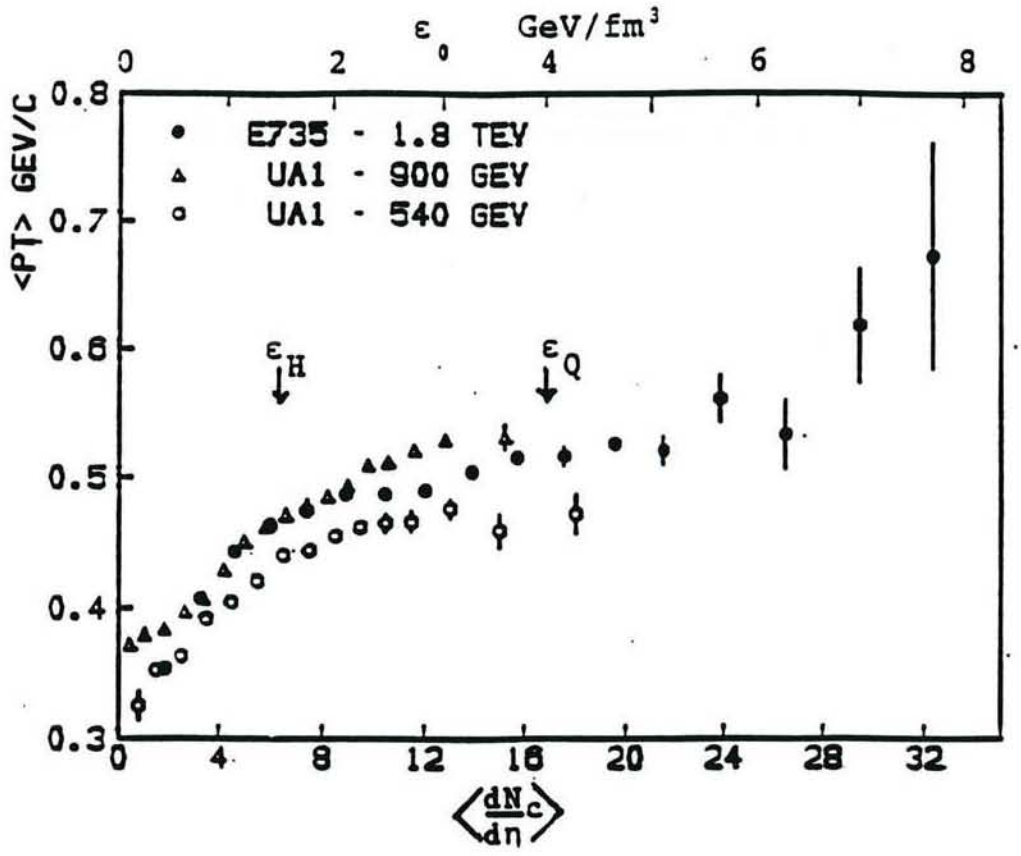

Fig. 1 Average transverse momentum of negative prongs versus multiplicity density in pseudorapidity (E-735[3]).

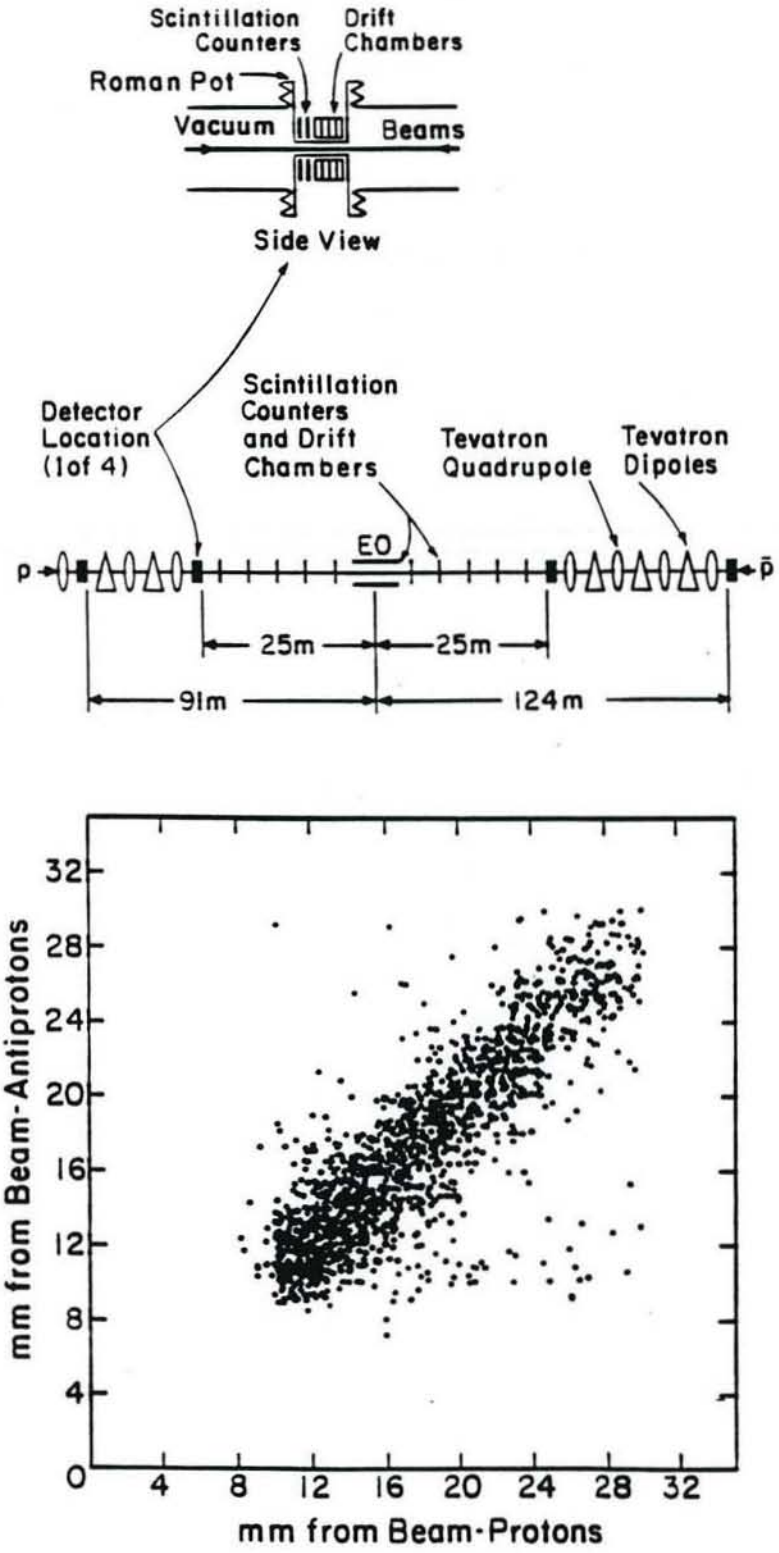

Fig. 2 E710 layout (top), and left-right correlation of track displacement, showing evidence for elastic events.

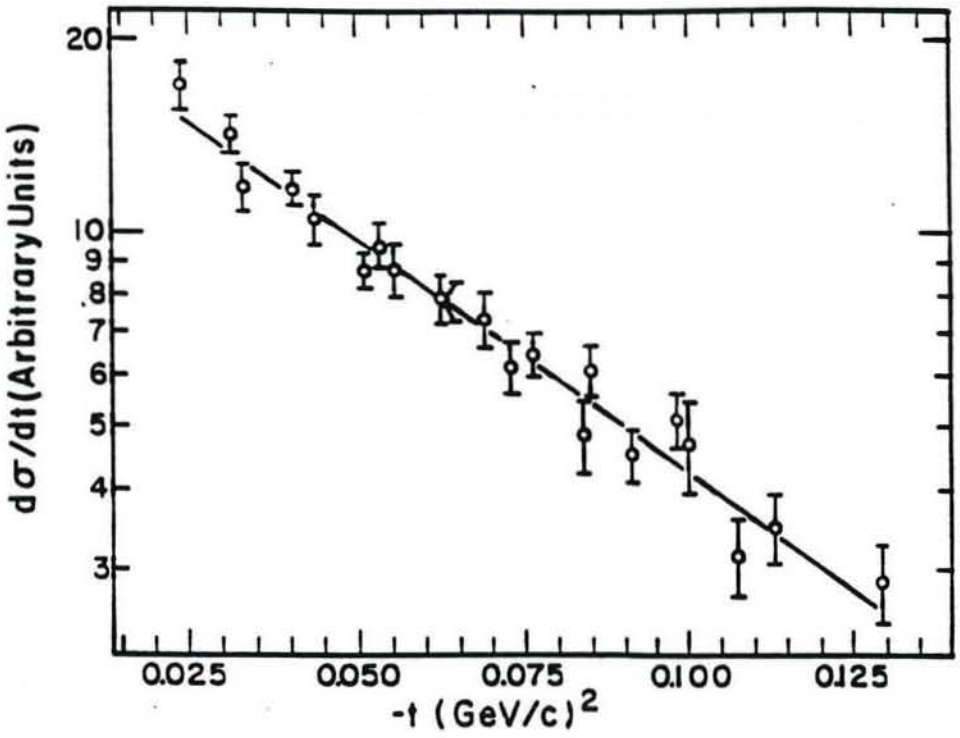

Fig. 3 E710 t-distribution of elastic events in proton-antiproton scattering at $\sqrt{s}$ = 1800 GeV[5].

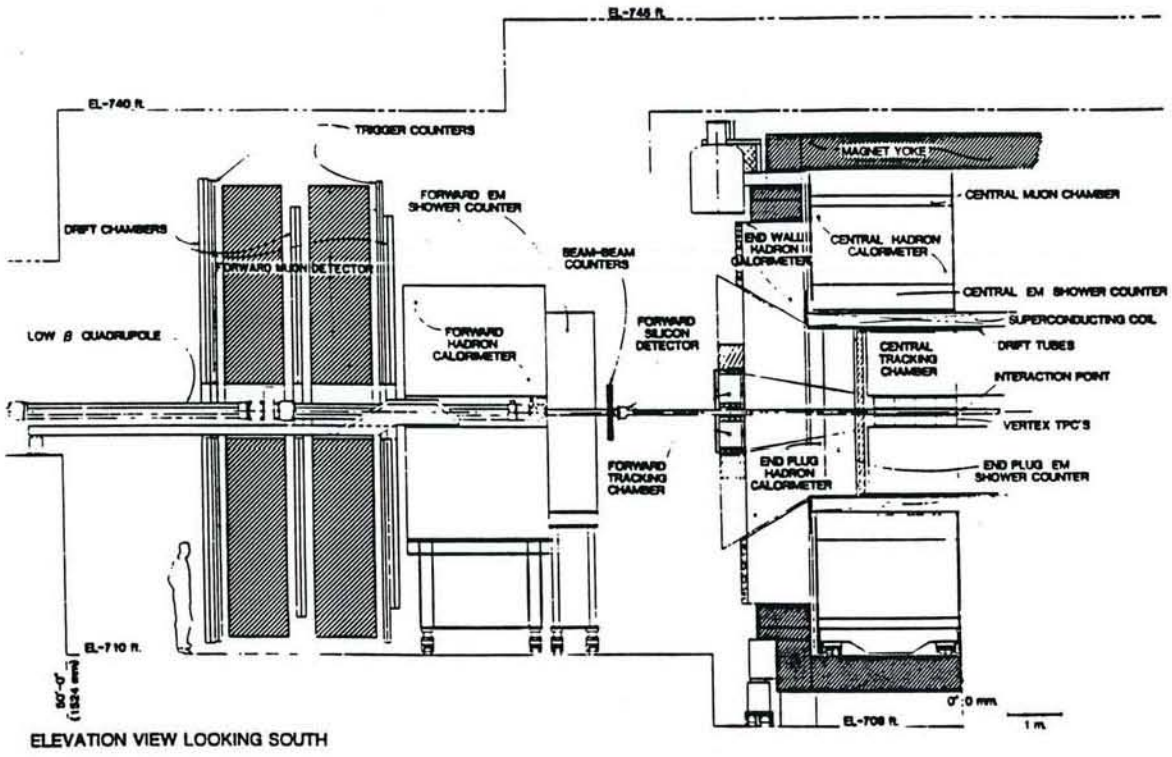

Fig. 4 A cut-away view through one half of CDF.

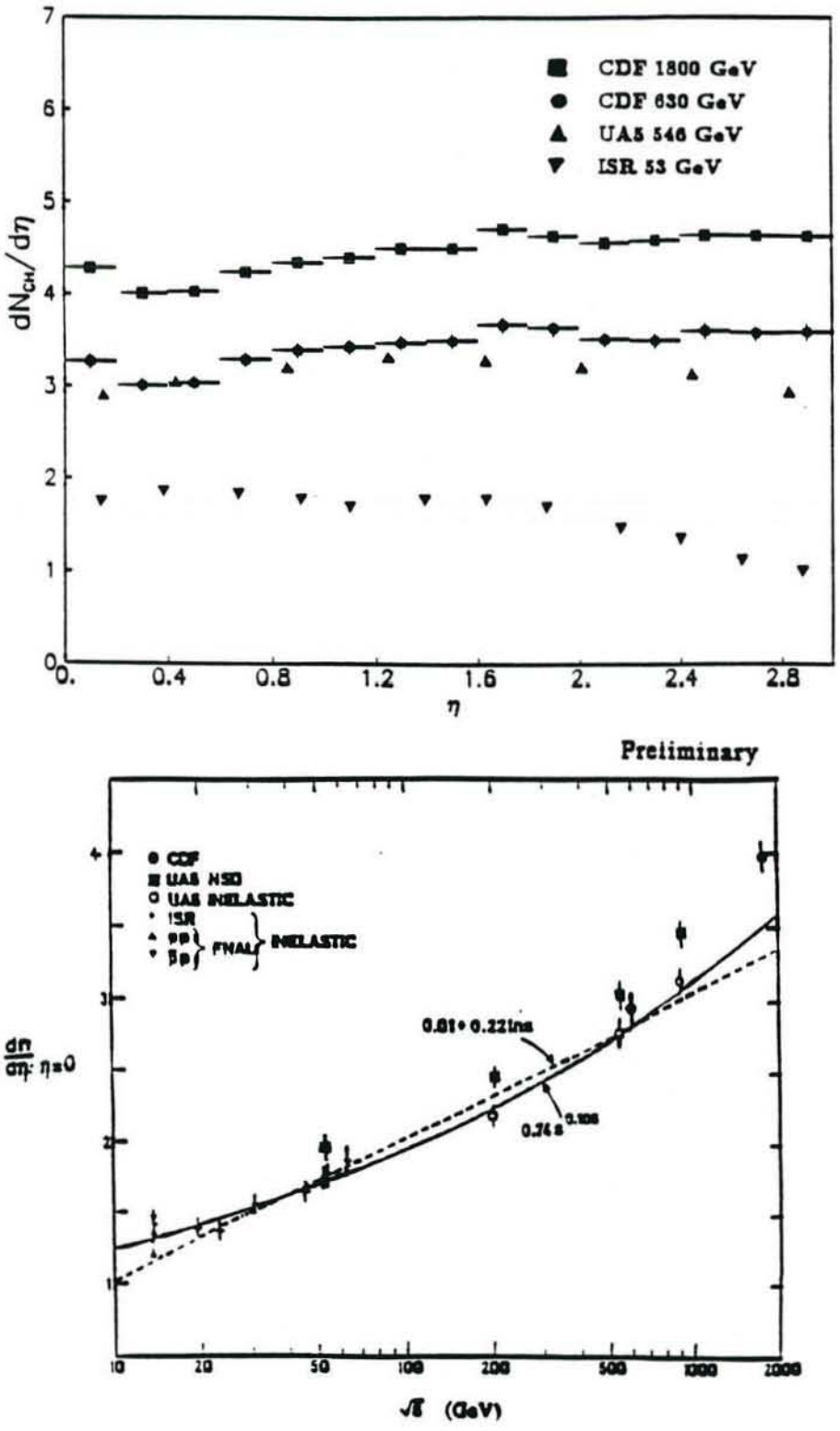

Fig. 5 Preliminary uncorrected pseudorapidity distributions measured at CDF[8].

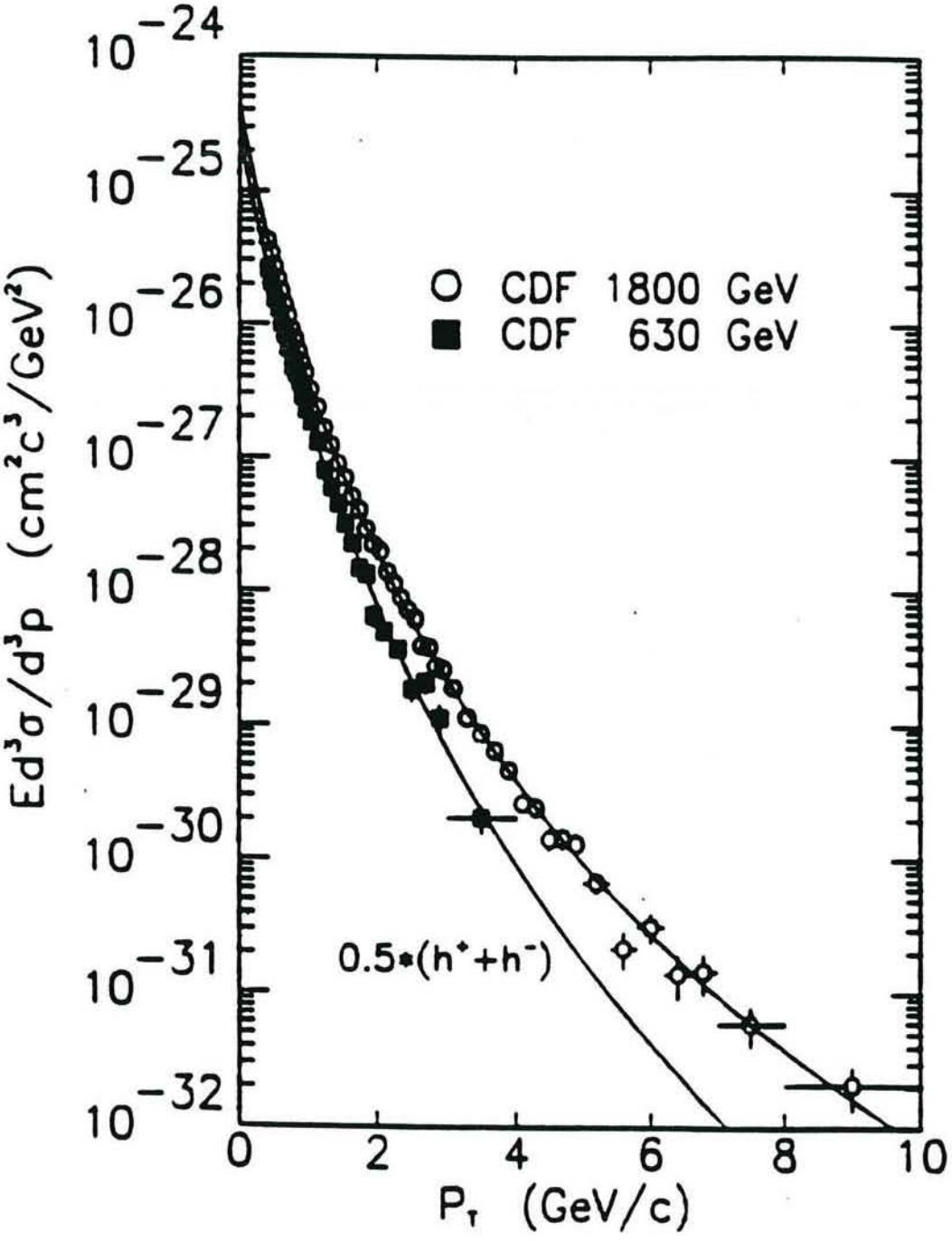

Fig. 6 Single charged particle inclusive cross-section for rapidity $|y| < 1.0$ and fitted curves with p_o fixed at 1.3 GeV/c[9].

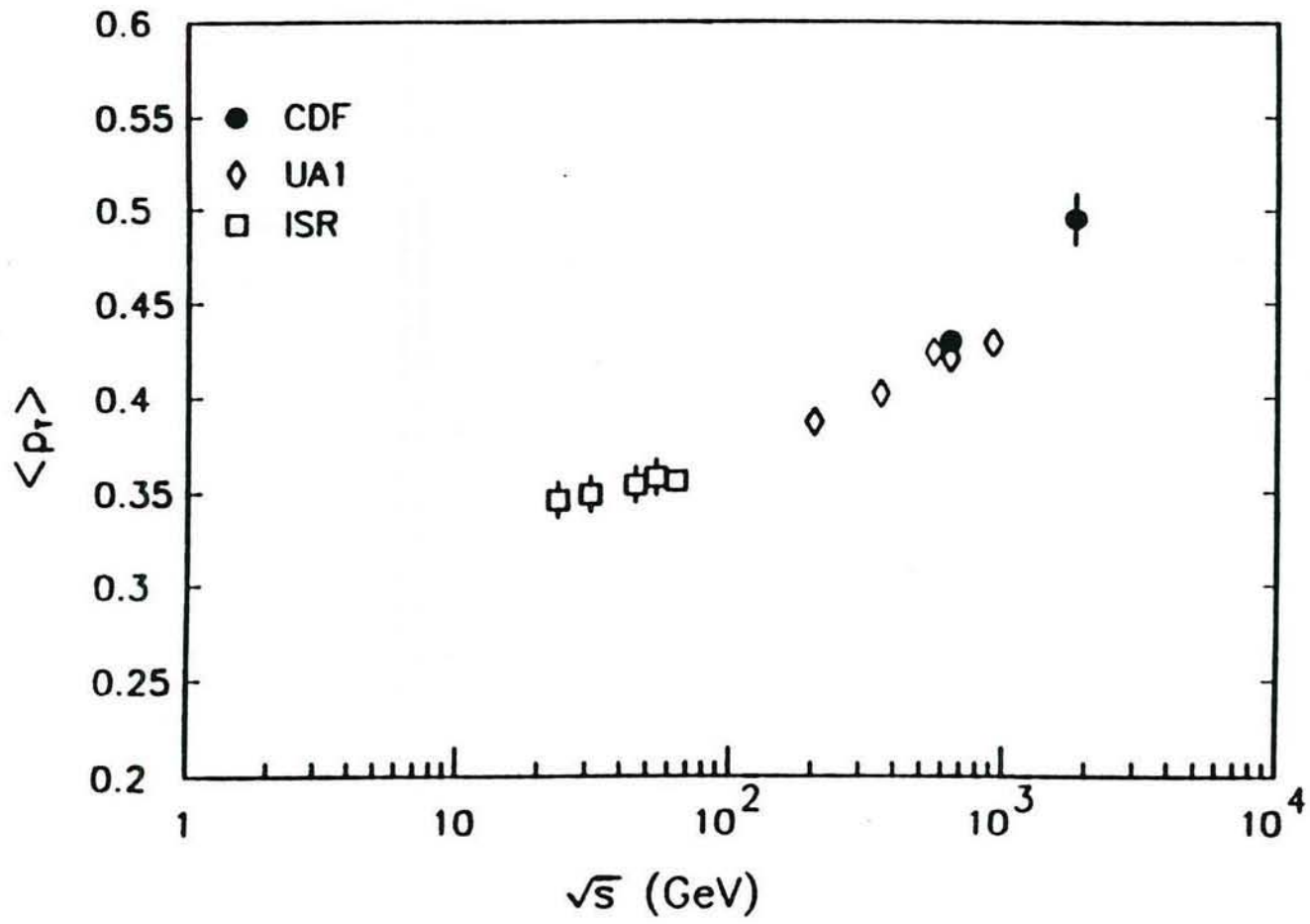

Fig. 7 Energy dependence of $\langle p_T \rangle$, from the ISR to CDF.

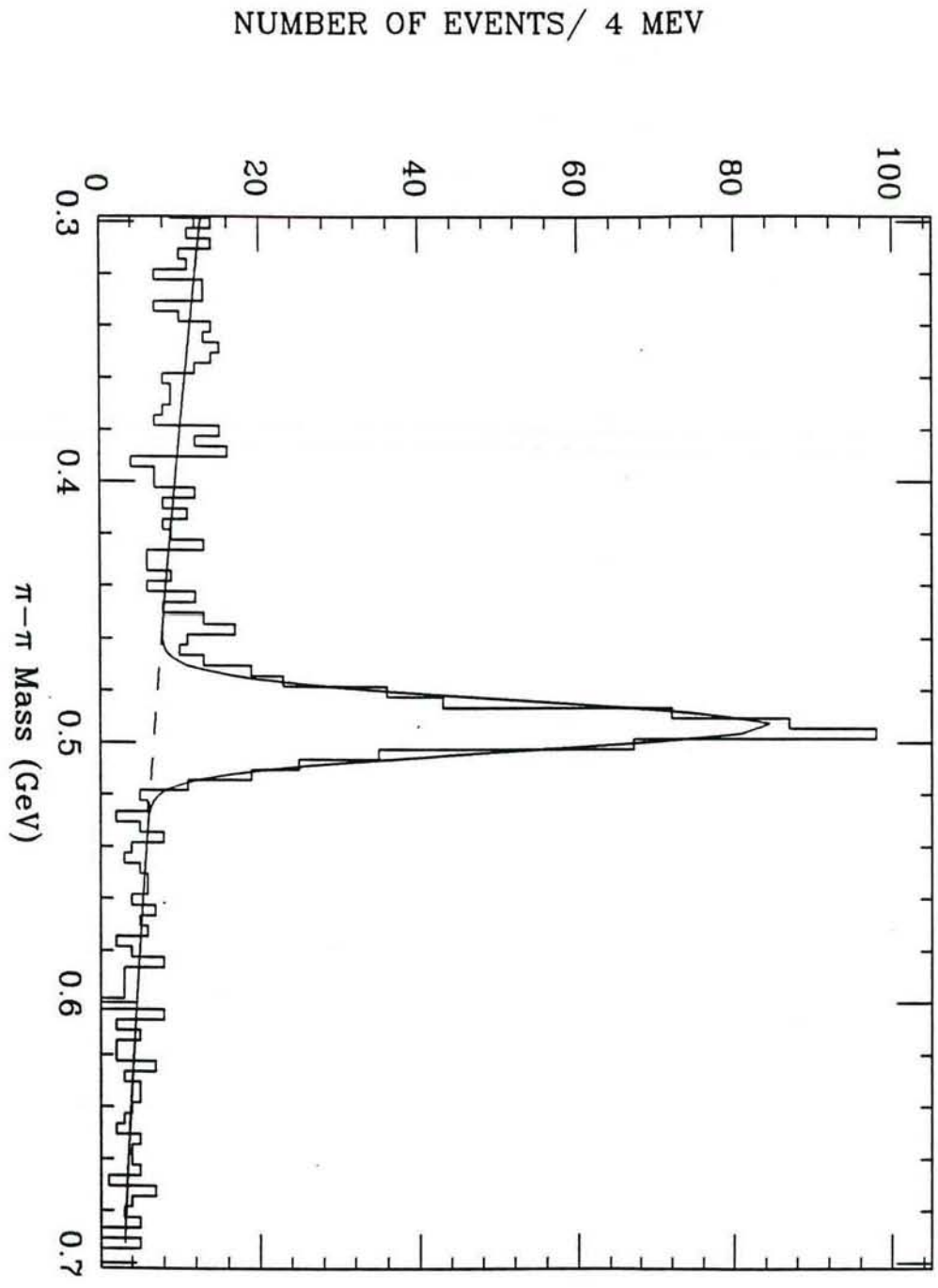

Fig. 8 Invariant mass-distribution of opposite charge particle pairs measured in the CDF CTC showing the K_o peak(8)(10).

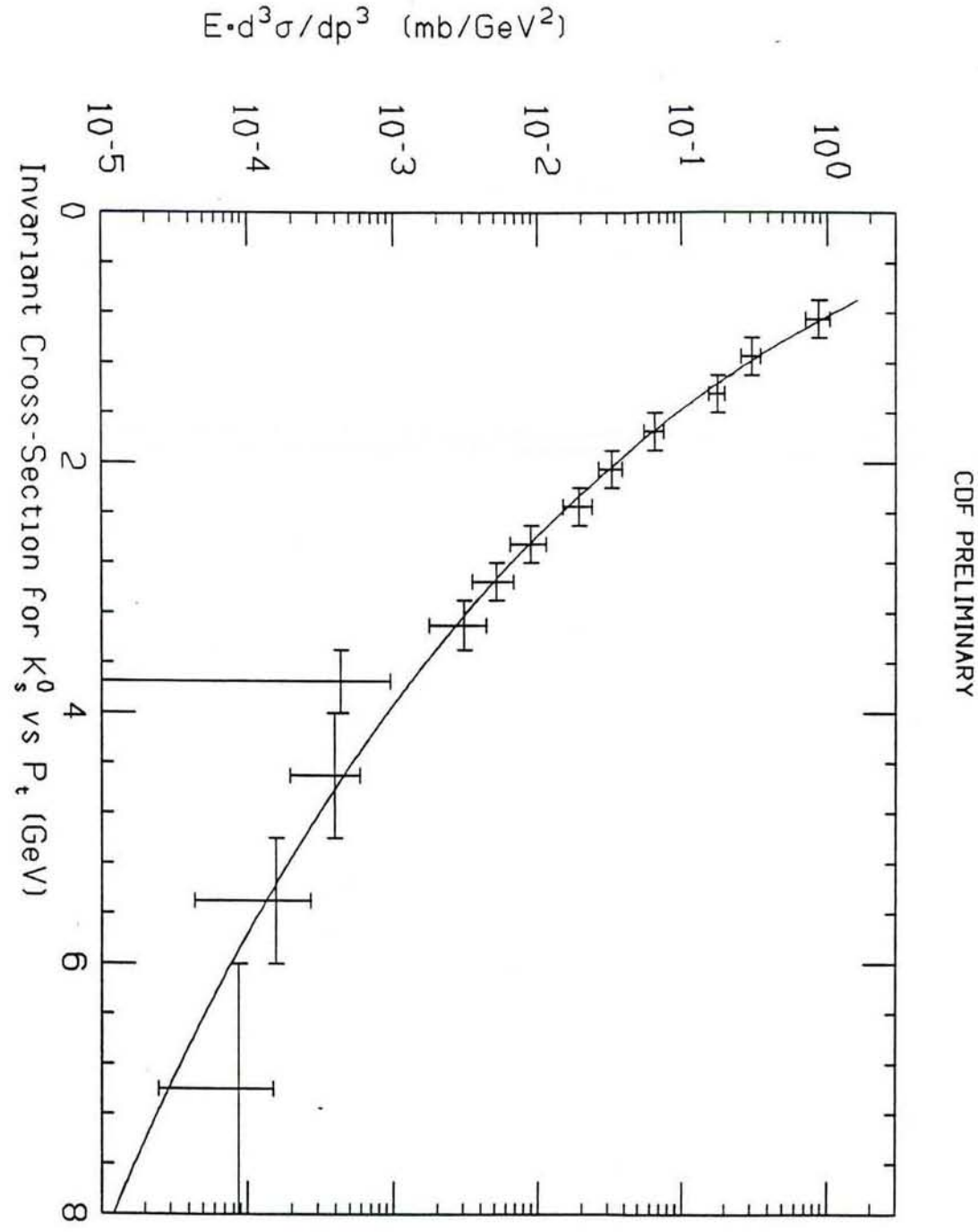

Fig. 9 Invariant cross-section for K_0-production (CDF 1987 data)[10].

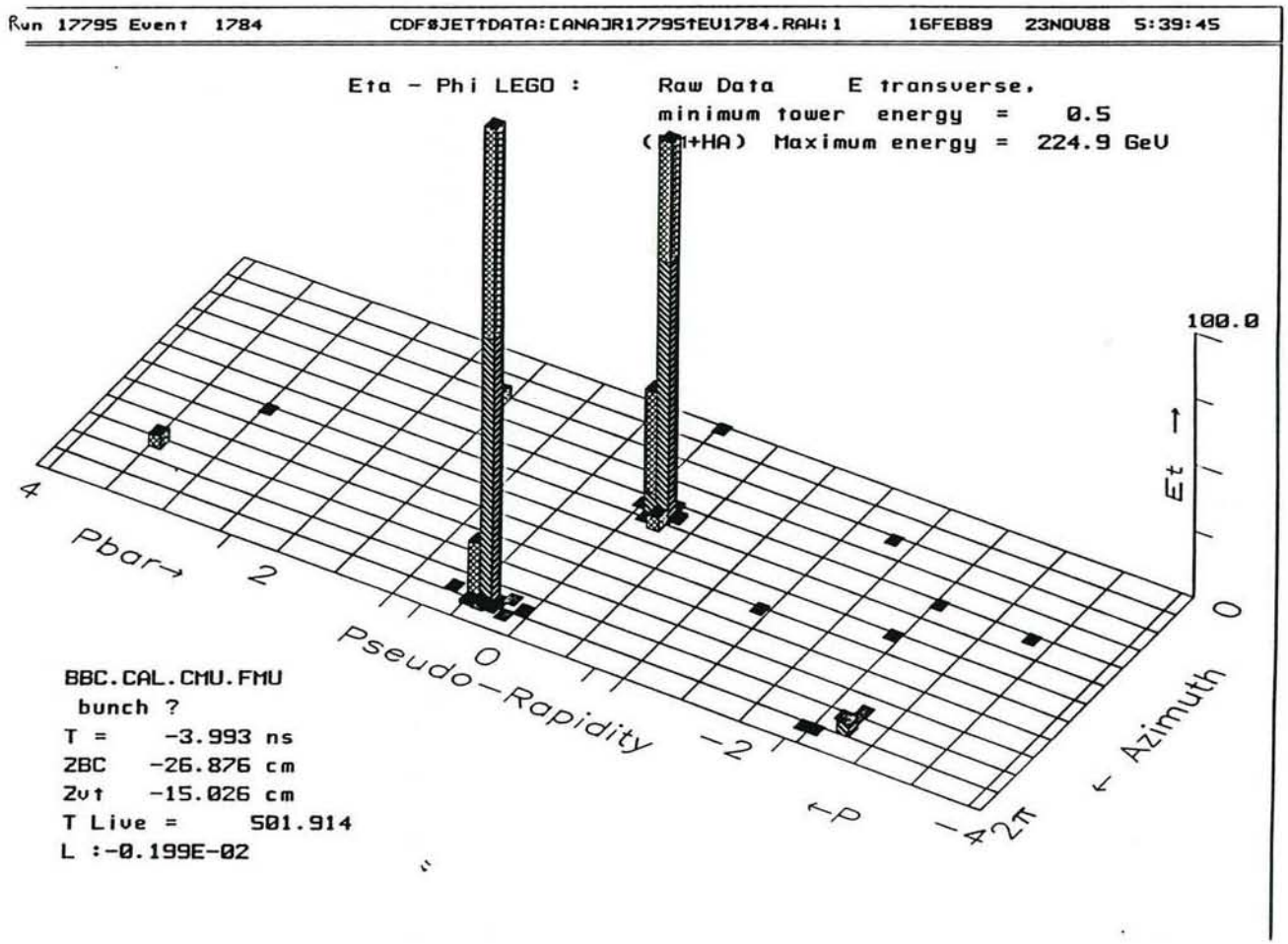

Fig. 10 Typical CDF jet event, as seen in the "Lego plot".

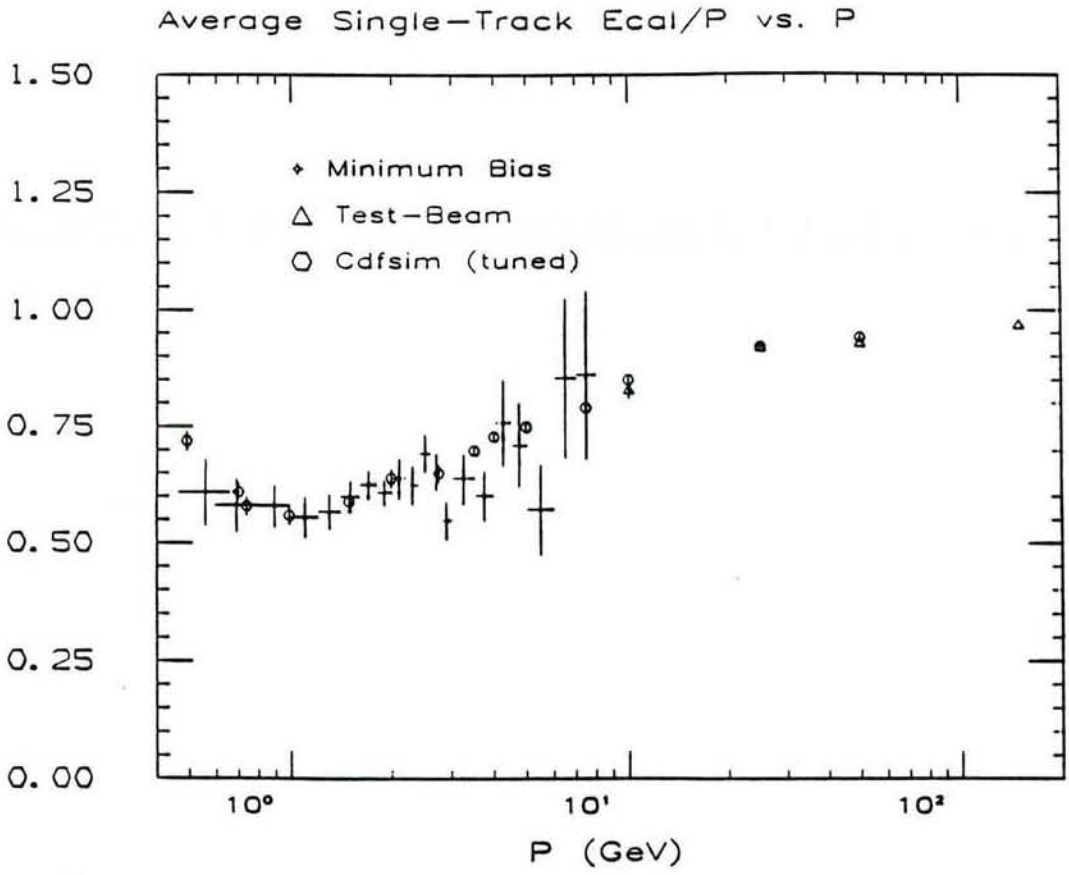

Fig. 11 Energy dependence of response of CDF central calorimeter to charged isolated hadrons.

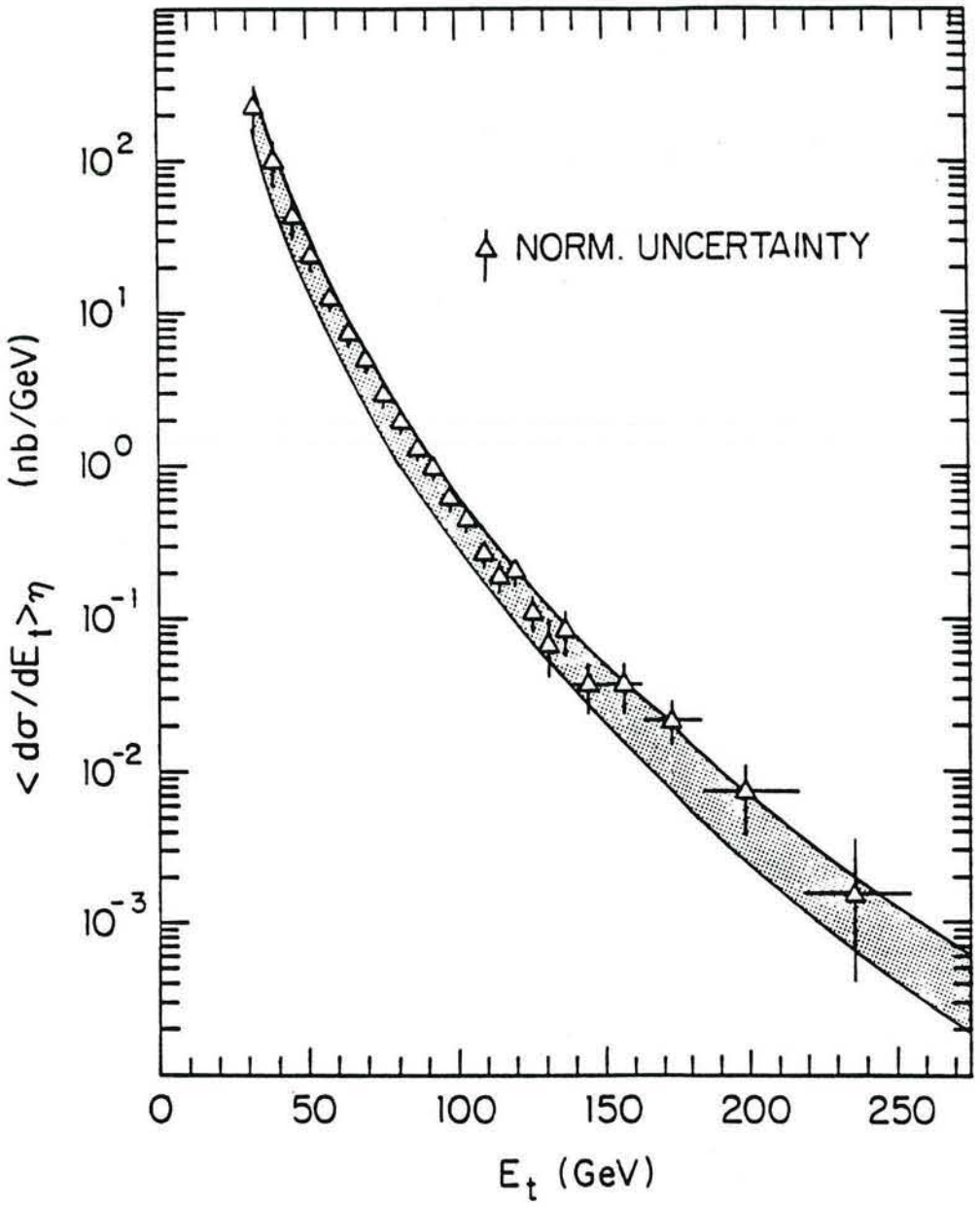

Fig. 12 The CDF inclusive central jet cross-section at $\sqrt{s}$ = 1800 GeV as a function of transverse energy compaired to a range of QCD predictions.

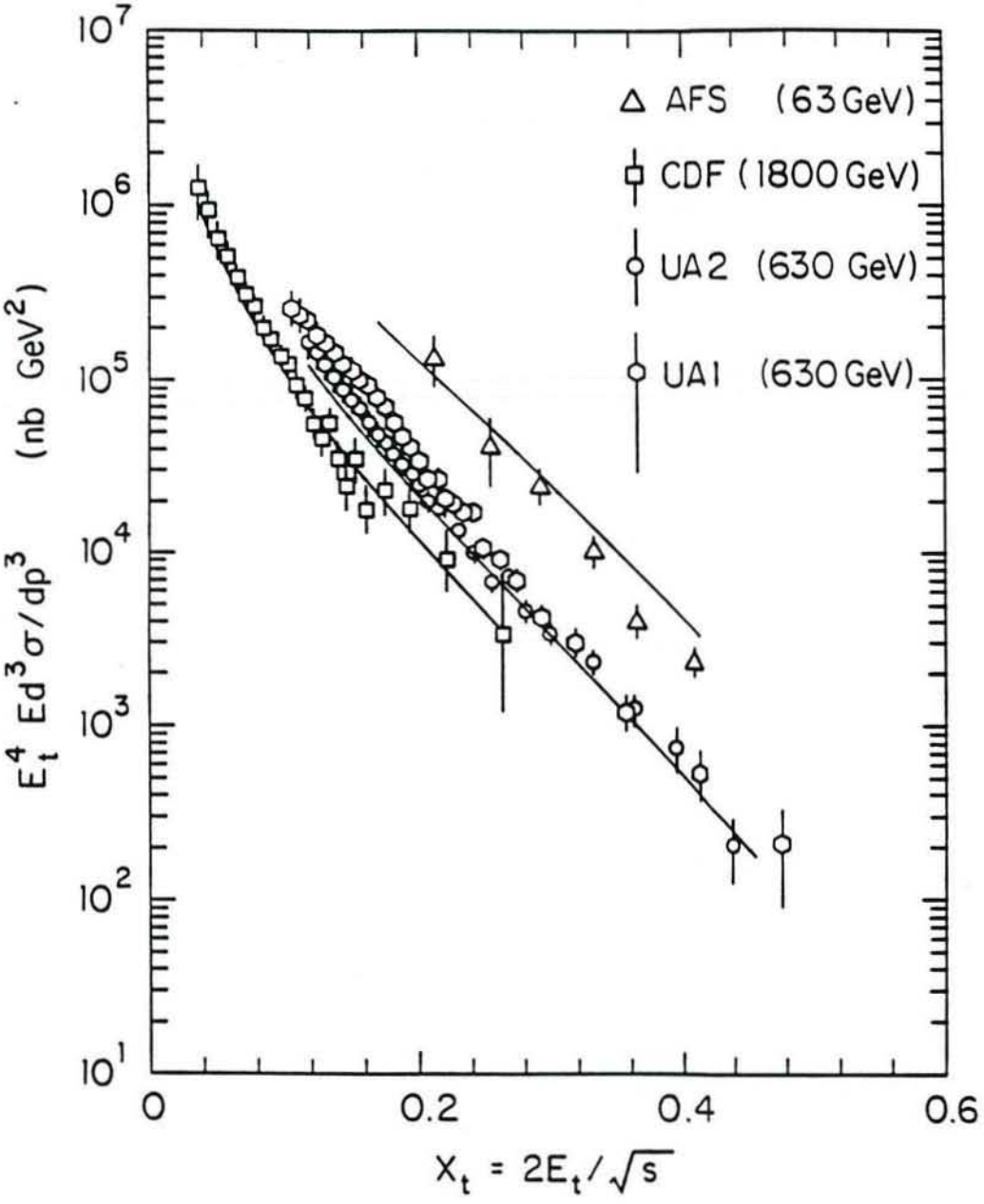

Fig. 13 Scaled jet cross-section[20] as a function of $x_t = 2\,E_t/\sqrt{s}$ for the UA1, UA2 and CDF experiments. Also shown are QCD predictions.

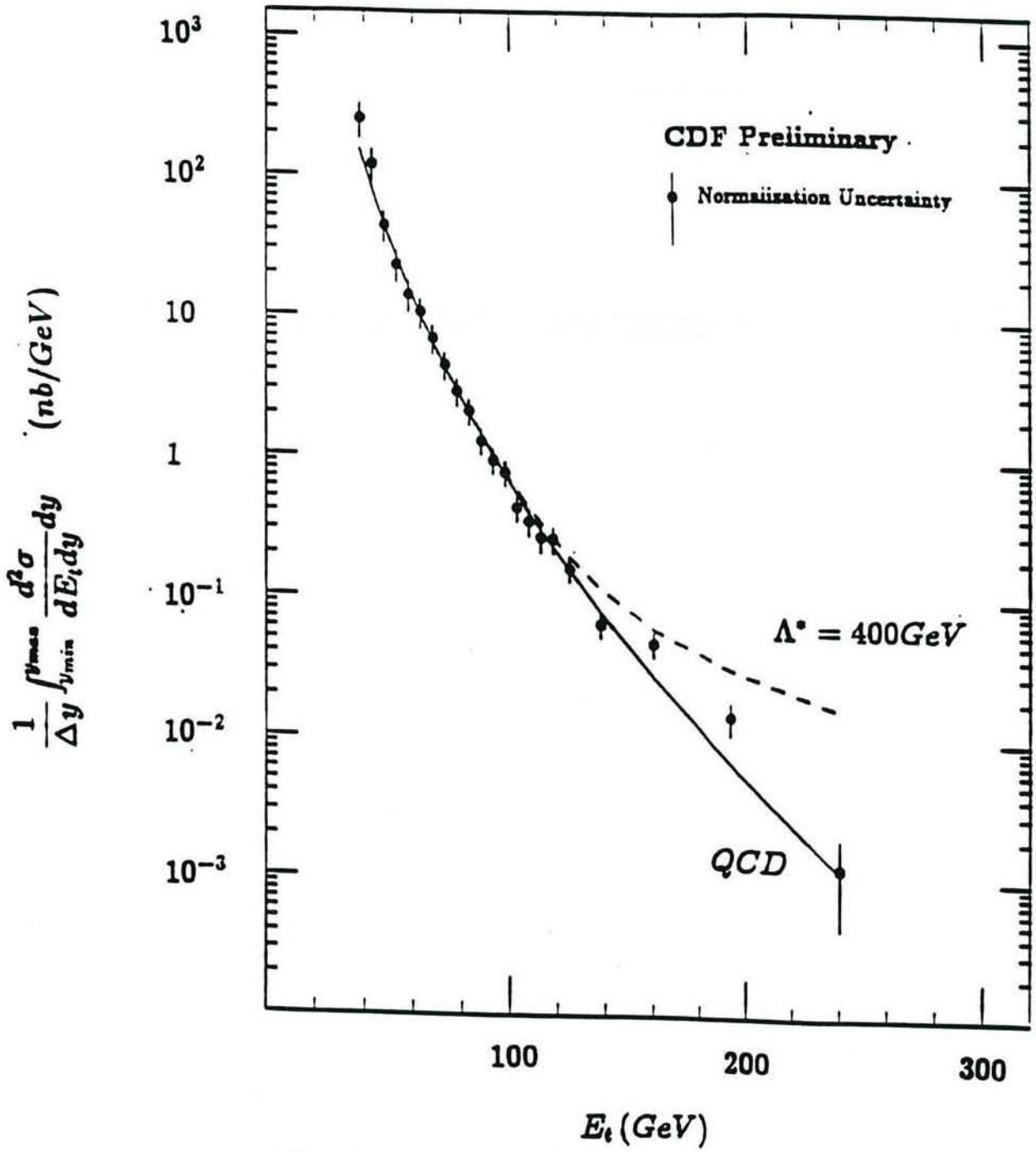

Fig. 14 CDF jet cross-section at $\eta = 0$, as a function of E_T. The large E_T tail is compaired to the prediction if a contact term[21] with $\wedge = 400$ GeV (UA1 lower limit) is added to the QCD contribution.

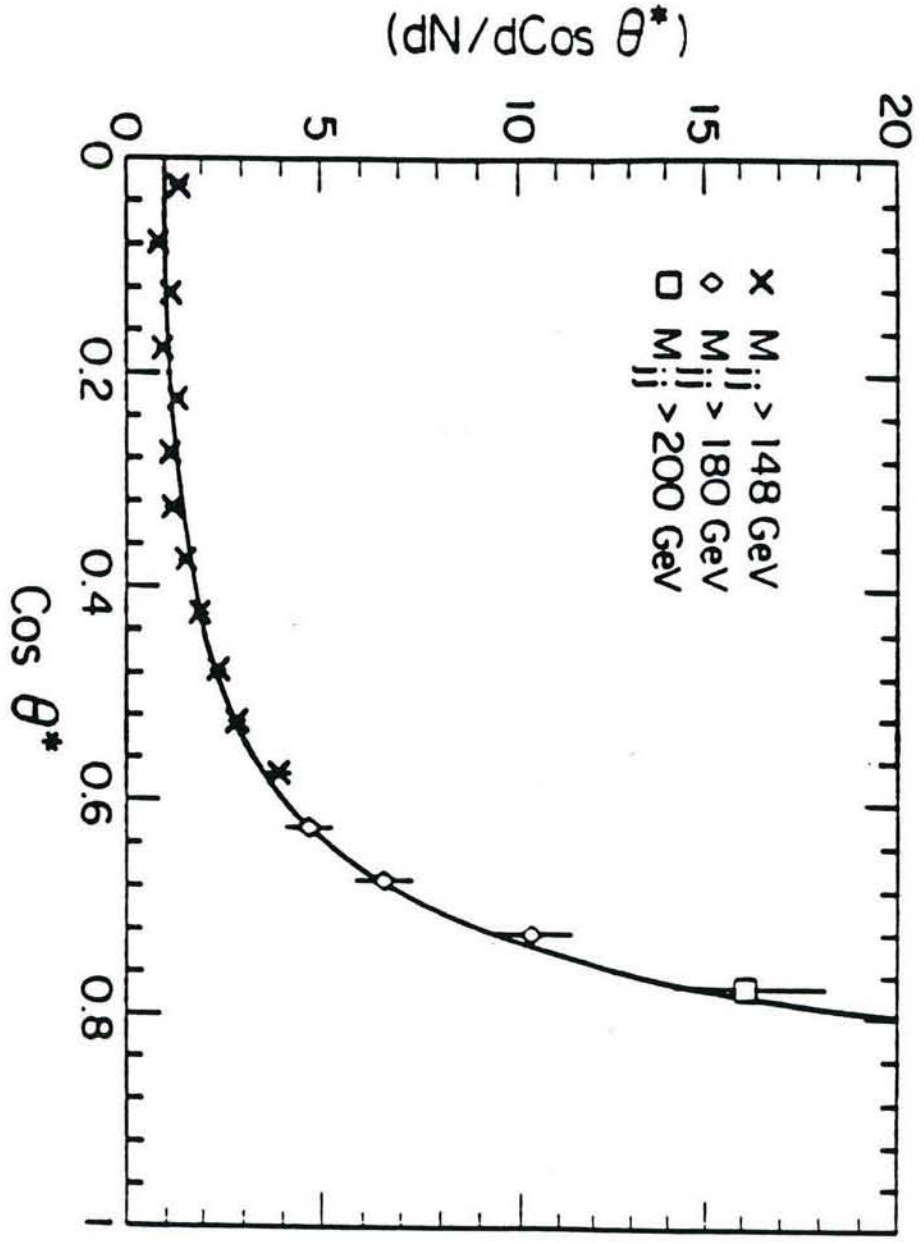

Fig. 15 Angular dependence of two jets cross-section in the jet cms (CDF data from 1987 run, ref.[22]).

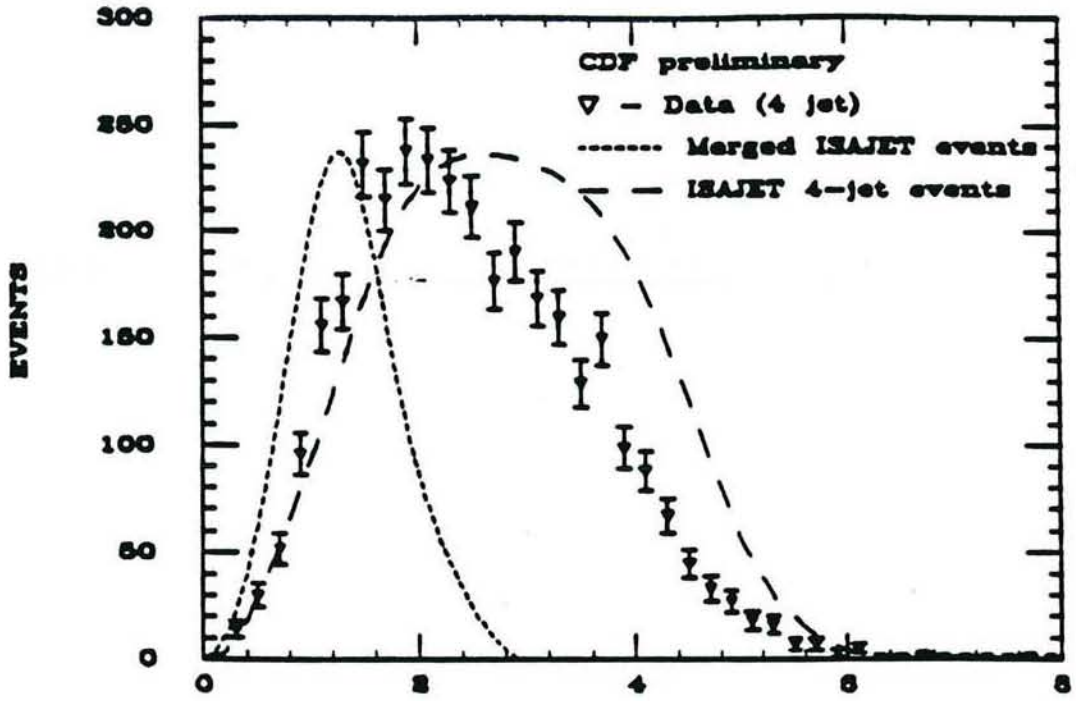

$$S = \sqrt{0.5\left(\frac{|\vec{E}_{t1} + \vec{E}_{t2}|^2}{|E_{t1}| + |E_{t2}|} + \frac{|\vec{E}_{t3} + \vec{E}_{t4}|^2}{|E_{t3}| + |E_{t4}|}\right)}$$

Fig. 16 Distribution of four-jet events versus the "paired missing E_T significance" (CDF preliminary data from 1987 run[23]). The data is compaired to expectation from overlap of two-jet events and from an approximate QCD Montecarlo of double gluon bremsstrahlung.

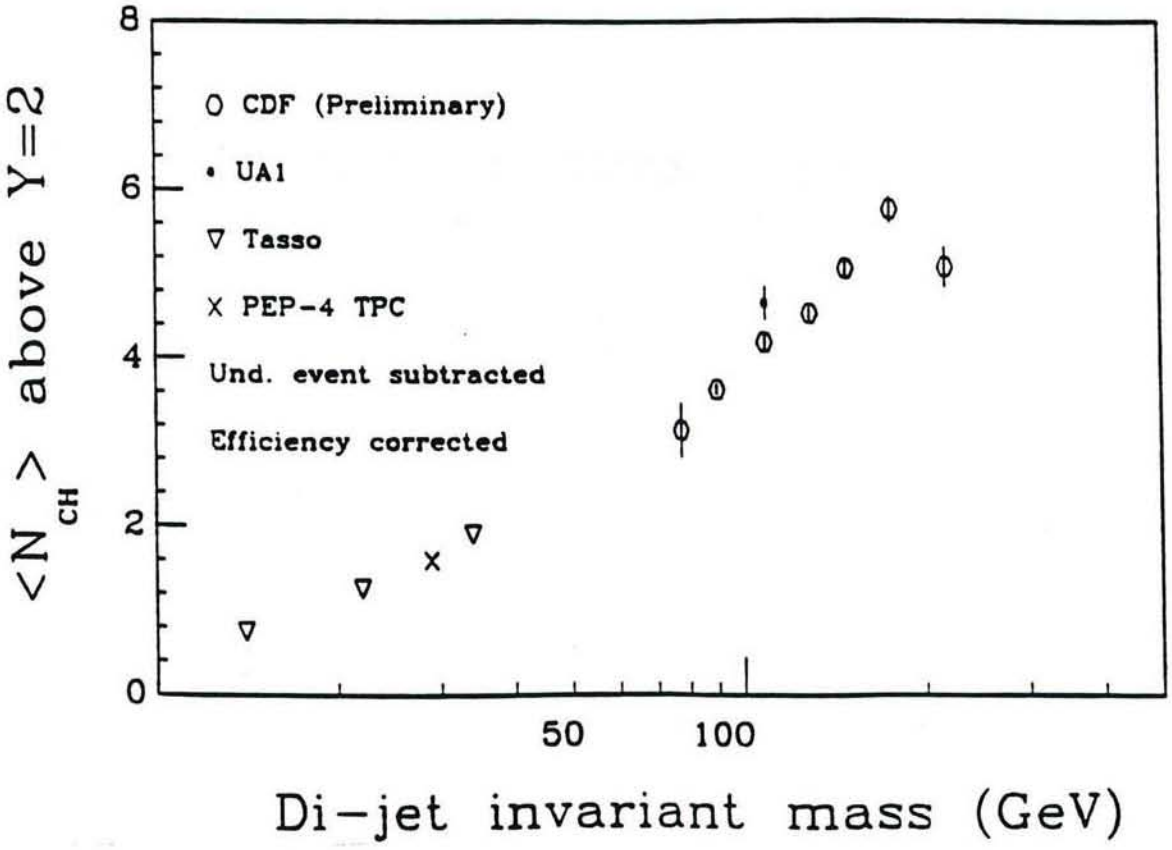

Fig. 17 Prong multiplicity in jet core ($\eta_j > 2$) as measured in CDF (preliminary result from 1987 run[24], compaired to e^+e^- data at lower dijet masses).

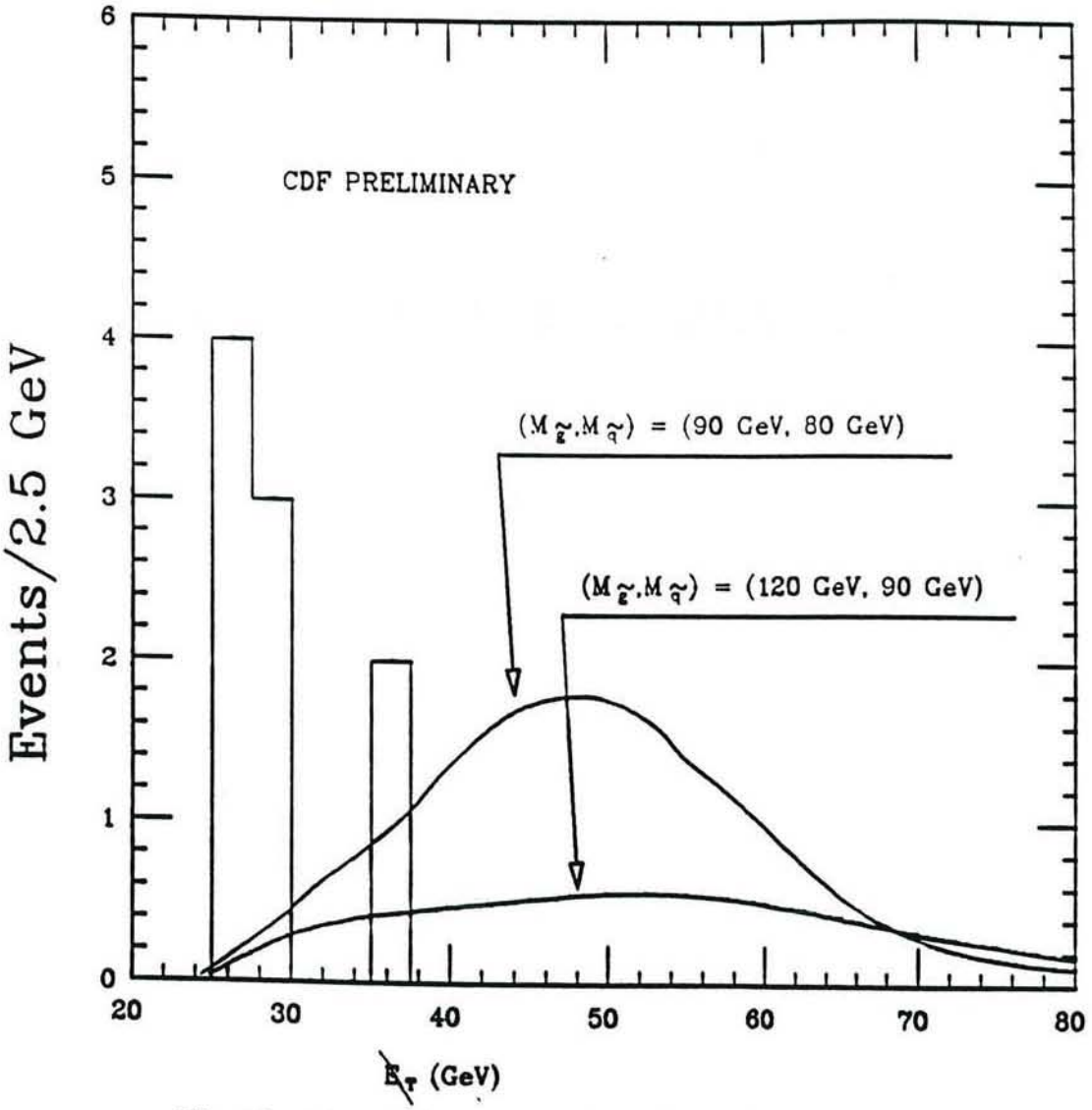

Fig. 18 Expected E_T distribution of monojet events for squarks and gluinos of masses around 100 GeV, compaired to 1987 CDF data[25].

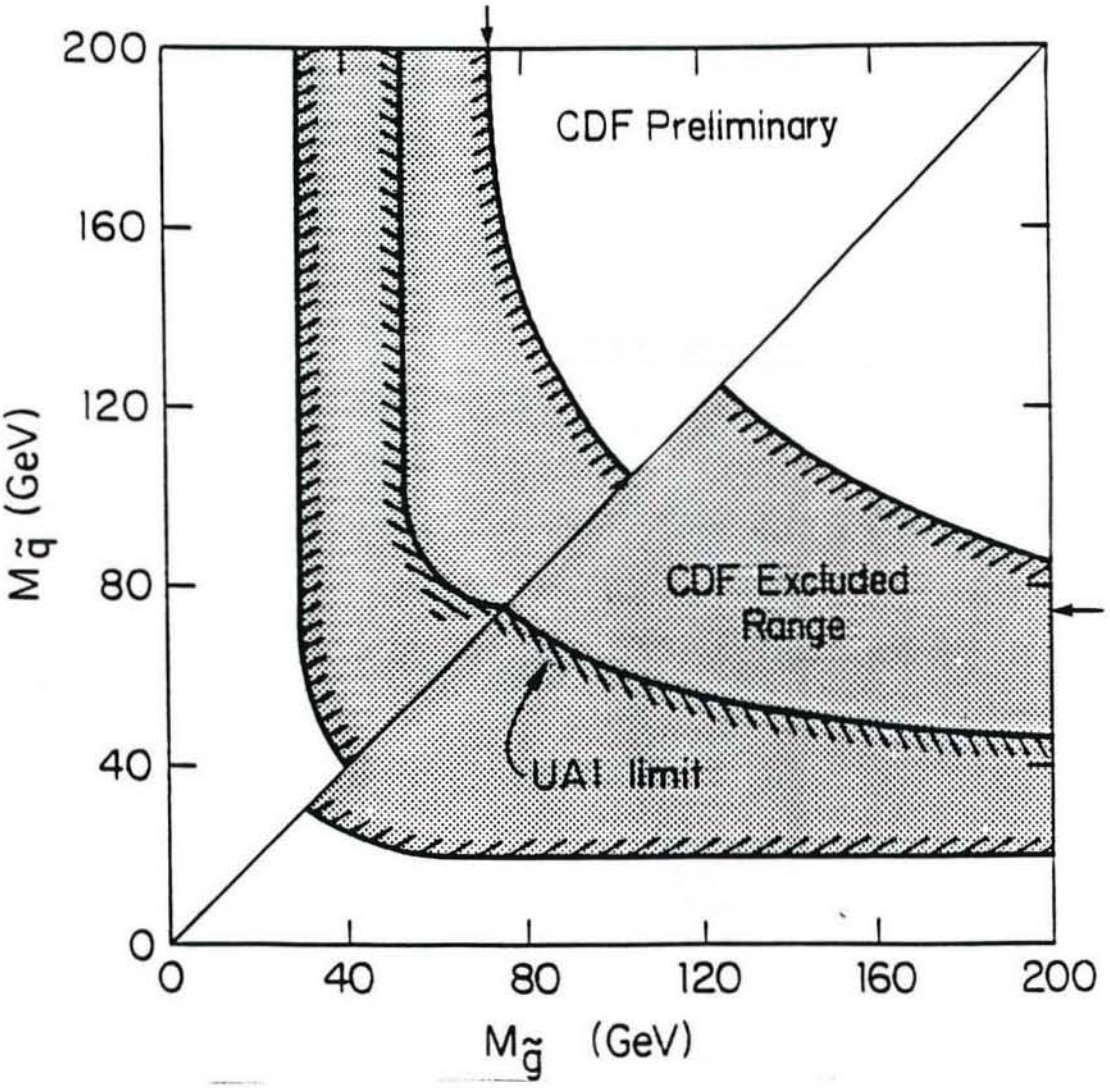

Fig. 19 Preliminary SUSY limits as derived from the CDF 1987 data.